

Control of neuronal network organization by chemical surface functionalization of multi-walled carbon nanotube arrays.

Jie Liu, Florence Appaix, Olivier Bibari, Gilles Marchand, Alim-Louis Benabid, Fabien Sauter-Starace, Michel De Waard

▶ **To cite this version:**

Jie Liu, Florence Appaix, Olivier Bibari, Gilles Marchand, Alim-Louis Benabid, et al.. Control of neuronal network organization by chemical surface functionalization of multi-walled carbon nanotube arrays.. Nanotechnology, 2011, 22 (19), pp.195101. 10.1088/0957-4484/22/19/195101 . inserm-00587525

HAL Id: inserm-00587525

https://inserm.hal.science/inserm-00587525

Submitted on 20 Apr 2011

HAL is a multi-disciplinary open access archive for the deposit and dissemination of scientific research documents, whether they are published or not. The documents may come from teaching and research institutions in France or abroad, or from public or private research centers.

L'archive ouverte pluridisciplinaire **HAL**, est destinée au dépôt et à la diffusion de documents scientifiques de niveau recherche, publiés ou non, émanant des établissements d'enseignement et de recherche français ou étrangers, des laboratoires publics ou privés.

Control of neuronal network organization by chemical surface functionalization of multi-walled carbon nanotube arrays

Jie Liu [1] , Florence Appaix [2] , Olivier Bibari [1] , Gilles Marchand [1] , Alim-Louis Benabid [1] , Fabien Sauter-Starace [1 *] , Michel De Waard [2 *]

[1] *CEA LETI CEA , CEA / Léti 17 rue des Martyrs 38054 Grenoble cedex 9,FR*

[2] *GIN, Grenoble Institut des Neurosciences INSERM : U836 , CEA , Université Joseph Fourier - Grenoble I , CHU Grenoble , UJF - Site Santé La Tronche BP 170 38042 Grenoble Cedex 9,FR*

* Authors to whom correspondence may be addressed: Michel De Waard <michel.dewaard@ujf-grenoble.fr > Fabien Sauter <fabien.sauter@cea.fr >

Abstract

Carbon nanotube substrates are promising candidates for biological applications and devices. Interfacing of these carbon nanotubes with neurons can be controlled by chemical modifications. In this study, we investigated how chemical surface functionalisation of multi-walled carbon nanotube arrays (MWNT-A) influences neuronal adhesion and network organization. Functionalisation of MWNT-A dramatically modifies length of neurite fascicles, cluster interconnection success rate, and percentage of neurites that escape from the clusters. We propose that chemical functionalisation represents a method of choice for developing applications in which neuronal patterning on MWNT-A substrates is a must.

Introduction

Since the pioneering work realized in 1970s [1], brain-computer interfacing (BCI) research has blossomed in recent years [2]. BCI research activity focuses on the following three fields: i) real-time cerebral signal recording to better understand brain function [3 , 4], ii) neuronal stimulation in neuroprosthetics applications [5] for disease therapy and iii) damage restoring. In invasive BCI, capacitance current is employed during neuronal electric signal detection and neuronal stimulation. To gather more electrical information, electrode surfaces need to be enlarged to the point that it may create brain damage during implantation and decrease the accuracy of the targeting. One possible solution to solve this issue is the use of electrodes with nanostructured surfaces. Amongst various technologies for electrode surface nanostructuration, carbon nanotubes (CNT) have been successfully used since electrodes coated with CNT show improved neuronal signal recordings [6 ,7]. CNT possess high electrical conductivity, excellent chemical stability and great mechanical resistance. They represent therefore promising materials in biotechnology and biomedication [8 ,9], especially in neuroscience [10]. In addition, nanotube arrays promote surface softness that has been demonstrated to favor neuronal growth [11 ,12].

From the various studies conducted so far, CNT have been considerate as biocompatible substrates. Intraperitoneal, nasal or oral injection of CNT in mice appears to not cause signs of distress or tissue alterations [13]. However, not all reports are as encouraging as this one because the fiber-like shape of CNT was reported to stimulate inflammation and produce cancer [14]. In vitro , CNT appear as non toxic and support the attachment, spreading and growth of mammalian cells [15] (but see conflicting report [16] indicating the need for standardized toxicity tests [17]). In vitro experiments have shown that CNT substrate can promote neuronal growth and facilitate signal transmission [18 –21]. This observation opens many possible applications in neuroscience, such as i) regeneration of neuronal connections, ii) devices to stimulate and record from neuronal networks, and iii) micropatterning to influence and study neuronal morphology and/or neural networks. In the future, additional applications may include: i) delivery of bioactive molecules [22], and ii) coupling to MRI agents [9]. In spite of these exciting applications, there are only a few studies that have investigated the relationship between CNT and neurons in vitro [23 ,24]. Even less information is available on how chemical modification of CNTs may influence CNT/neuronal interaction. Data available indicate that chemical functionalization of CNT has the ability to influence neuronal morphology. Neurons grown on 4-hydroxynonenal-functionalized CNT substrate have multiple neurites and extensive branching, whereas neurons extend only one or two neurites with little branching on raw CNT substrate [25]. Xie et al . have also observed that oxidation of CNT mats promotes cell adhesion and neurite extension [26]. Precise control of neurite outgrowth and branching can be performed on CNT substrates functionalized by positively charged, negatively charged or neutral molecules [24 ,27]. Recently, Malarkey and collaborators showed that neurite outgrowth is influenced by the conductivity of PEG_{5000} -functionalized CNT film [28]. These studies indicate that chemical functionalisation of CNT may largely influence the relationship between CNT and neurons in vitro. However, these studies have focused mainly on the morphology of individual neurons after short times of culture (1 to 3 days) and have not addressed the influenced of CNT chemistry on collective neuronal behavior.

Here, we investigated the effect of chemical functionalisation of multi-walled carbon nanotube arrays (MWNT-A) on neuron adhesion and on the establishment of neuronal networks. Both non-covalent and covalent modifications have been studied since these treatments are expected to differ in their impact on MWNT-A conductivity, mechanical resistance and yield of functionalization according to earlier reports on single nanotubes. PEG_{5000} functionalization of MWNT-A has also been performed using PEG_{5000} because it is known to reduce

non specific protein adsorption at the surface of the nanotubes [29]. Treating MWNT-A by different chemistries, we demonstrate that the organization of neurons at the surface of MWNT-A substrates largely evolves with time in culture reflecting cell motility and clustering processes. We found that non-functionalized MWNT-A possess good neuronal adhesion properties and favor a developed neuronal network with the formation of clusters of neuronal bodies comprising some local neurites and fascicles of neurites that connect neighboring clusters. Chemical functionalisation greatly influences the neuronal network adhesion and organization. From these studies, we conclude that chemical functionalisation may be used to create neuronal patterns at the surface of MWNT-A substrates.

Experimental and methods

Synthesis of MWNT-A on silicon substrate

MWNT-A were grown on silicon wafer coated with i) a layer of silicon oxide (SiO_2 , 1 μm thick), followed by ii) a layer of titanium nitride (TiN, 300 nm thick) and iii) a layer of nickel (5 nm). The SiO_2 layer was deposited by chemical vapor deposition (CVD), whereas layers of TiN and nickel (5 nm) were deposited by sputtering. The nickel layer acts as catalyst for CNT growth; growth that occurs at 600° C by CVD in an atmosphere composed of acetylene and hydrogen at low pressure during 15 min. Figure 1(A) schematically describes the substrate nanostructured by MWNT. As shown by scanning electron microscopy (SEM) images, the growth of the MWNT occurs randomly regarding their orientation (figure 1(B)). The average diameter and length of the MWNT is about 50 nm and 1.5 μm, respectively. The entire surface of the substrate is covered by MWNT as witnessed by a vertical SEM view. The silicon wafer with raw MWNT-A (MWNT-A_0) was diced into 10×10 mm samples for further chemical functionalisation and/or cell cultures.

Chemical functionalisation of MWNT-A

Five different chemistries were used to functionalize MWNT-A_0 (figure 1(C)). MWNT-A_1 were prepared by incubation of MWNT-A_0 in an aqueous solution of trimethyl-(2-oxo-2-pyren-1-yl-ethyl)-ammonium bromide [30] (**1** , 1 mM) for 24 hrs, rinsing by H_2O and dried in vacuum at room temperature. MWNT-A_2 and MWNT-A_3 were prepared similarly with different incubation solutions: 1-pyrenebutyric acid [31] (**2** , 2 mM) in 0.1 M sodium tetraborate (STB) buffer solution (pH 9.2) (MWNT-A_2) or pyrene-PEG_{5000} [29] (**3** , 2 mM) aqueous solution (MWNT-A_3). To prepare MWNT-A_4 , MWNT-A_0 was treated with O_2 plasma (O_2 flow rate: 20 sccm) with a 20 W power for 1 min. No reduction in the length of the MWNT-A was observed in scanning electron microscopy (SEM) at this power. MWNT-A_5 were prepared by incubation of MWNT-A_4 in an aqueous solution of amino-terminated PEG_{5000} (2 mM) in the presence of 1-ethyl-3-[3-dimethylaminopropyl]carbodiimide hydrochloride (EDC, 2.5 mM) for 18 hrs and rinsed thoroughly with H_2O. Next, the sample was dried in vacuum at room temperature. So MWNT-A_1 , MWNT-A_2 and MWNT-A_3 were non-covalently functionalized by positively charged trimethyl-(2-oxo-2-pyren-1-yl-ethyl)-ammonium (MWNT-A_1), negatively charged 1-pyrenebutyric acid (MWNT-A_2) or by pyrene-PEG_{5000} (MWNT-A_3), respectively. Conversely, MWNT-A_4 was covalently modified by plasma oxygen treatment yielding a mixture of carboxyl, carbonyl and hydroxide groups. MWNT-A_5 was developed on the basis of MWNT-A_4 by additional covalent coupling to PEG_{5000} .

The contact angles of H_2O on the functionalized surfaces are as follows: 152° (MWNT-A_0), 132° (MWNT-A_1), 134° (MWNT-A_2), 28° (MWNT-A_3), 0° (MWNT-A_4 and MWNT-A_5). Therefore, the most hydrophobic surfaces were MWNT-A_0 , MWNT-A_1 and MWNT-A_2 , whereas the hydrophilic ones were MWNT-A_3 , MWNT-A_4 and MWNT-A_5 . Differences in water contact angles between MWNT-A_2 and MWNT-A_4 (both with carboxylic groups), and between MWNT-A_3 and MWNT-A_5 (both with PEG_{5000} functionalization), are most likely due to the plasma treatment used for MWNT-A_4 and MWNT-A_5 , which also yields higher functionalization levels. A complete characterization of the various MWNT-A substrates is illustrated and described in Supplementary data (figure S1) .

Sterilization of MWNT-A samples

The MWNT-A samples are sealed in a double Tyvek package (provided by SüdPack Medica) then were sterilized after functionalization by MXM STERLAB using a short cycle of ethylene oxide exposure at a temperature between 45 and 55°C. Out-gazing is applied to the sample according to EN 550 and ISO EN 10993-7 standards to avoid the presence of ethylene oxide residues on the sample after sterilization. The absence of residual ethylene oxide is controlled by gas phase chromatography.

Primary neuronal cultures

Hippocampal neuronal cultures were prepared from E19 rat embryos using a modified protocol of Goslin and Banker [32]. Control condition corresponds to neurons seeded at a density of 1.5×10^4 per cm^2 on coverslips coated with poly-D-lysine (PDL, Poly-D-lysine hydrobromide, Sigma, Cat. No. P7280). Neurons were incubated in neurobasal medium containing B27 supplement (Gibco, Invitrogen). Hippocampal neurons were seeded on sterile MWNT-A samples at the same concentration as under the control condition, but without PDL coating. Cultures were maintained at 37°C in a 5% CO_2 incubator with neurobasal media supplemented with B27, 1 mM sodium pyruvate,

GlutaMAX™ (2 mM), penicillin/streptomycin (10 U/ml). Additional serum-free Neurobasal-B27 medium was added twice a week. Housing and handling of animals complied with the regulations issued by the European Union and INSERM and were approved by the GIN veterinary and ethics committee.

Sample preparations for studying neuronal patterning

Three types of MWNT arrays samples are prepared for neuronal patterning. MWNT-$A_{0/2}$ represents an array substrate in which one half of the surface corresponds to MWNT-A_0 and the other half to MWNT-A_2 . These arrays have a size of 10×20 mm. MWNT-$A_{4/5}$ similarly represent a 10×20 mm array substrate in which half of the array surface corresponds to MWNT-A_4 and the other half to MWNT-A_5 . Finally, MWNT-A_{5S} represent a 10×20 mm array substrate of the type MWNT-A_5 but on which manual scratches were performed with a needle in order to remove MWNT and to expose TiN substrate under the area of the scratch. SEM observation of the sample shows that the scratching procedures yields ditches with a width of about 5–10 μm between MWNT arrays.

Scanning electron microscopy (SEM)

For SEM observations, samples after neuronal culture were fixed for 15 min at room temperature in phosphate-buffered saline (PBS) with 4% paraformaldehyde (PFA). The fixed samples were then dehydrated by 10 min incubations in increasing concentrations of ethanol (70%, 80% and 90%), followed by three 10 minutes rinses with 100% ethanol. Next, the dehydrated samples were incubated in hexamethyldisilizane for 5 min and dried. Finally, samples were metalized by Pt and were examined using a Hitachi S-4100 scanning electron microscope.

Immunostaining and confocal microscopy

For cell immunostaining, samples were first washed with PBS and fixed with 4% PFA for 15 min. Next, they were permeabilized with 1% Triton® X-100 (Sigma) in PBS for 15 min and blocked with 5% Bovine Serum Albumin (BSA, fraction V, Sigma, Cat. No. A9647) for 30 min. Samples were incubated with primary antibodies in a solution containing 0.1% Triton X-100 and 3% BSA in PBS overnight at 4° C. To detect neuronal cells, 1:500 mouse anti-βIII tubulin (TUJ1) monoclonal antibody covalently coupled to Alexa Fluor® 488 (Covance, Cat. No. A488-435L) was used. The monomeric cyanine nucleic acid stain To-Pro®3 (Molecular Probes, Cat. No. T3605) was used to stain cell nuclei. Finally, samples were prepared using a mounting medium (Dako, Cat. No. S302380) and covered with a cover slip. The mounting medium was dried overnight at room temperature before fluorescence measurements. Images of stained cells were acquired by a confocal laser scanning microscope (Leica TCS SPE, Leica Microsystems, Heidelberg, Germany). Samples were scanned using a 10x/0.30 dry plan lens or a 40x/1.25-0.75 oil immersion lens. Excitation wavelengths used were 488 nm (TUJ1) and 635 nm (To-Pro®3).

Statistical analyses

Fascicles of neurites were defined as an assembly of more than 5 neurites. A neurite was considered as having a diameter of 1 μm, whereas the smallest fascicles of neurites were considered having a diameter close to 3 μm. Neuron clusters comprise a minimum of 10 cell soma. Clusters too small (less than 40 μm in diameter) to be distinguished from individual cell soma (up to 15 μm of diameter) were discarded from the analyses. Paired t -tests were performed where necessary. NS, non-significant; *, $p < 0.05$; **, $p < 0.01$; and ***, $p < 0.001$.

Results

Cultured neurons on MWNT-A after 3 days in vitro

Primary cultures of dissociated hippocampal neurons were first performed on a coverslip covered by PDL as a control sample. Neurons were identified by their characteristic pyramidal shape, tuj-1 immunoreactivity and the presence of neurites. After 3 days in vitro (DIV), hippocampal neuron cultures present significant cell densities (243 ± 41 cells/mm^2) (figure S2(A) in supplementary information). Next, primary neuronal cultures were seeded on both raw (MWNT-A_0) and functionalized MWNT-A (from MWNT-A_1 to MWNT-A_5) and observed after 3 DIV by fluorescence confocal microscopy (figure 2). For observation, neurons are stained with a specific neuronal β -tubulin III marker (Tuj-1, green) that labels the cytoskeleton. All cell types are visualized by staining with the monomeric cyanine nucleic acid stain To-Pro3® for cell nuclei observation (red). On all samples, the distribution of cells is homogeneous at the surface of the substrate indicating that all surfaces possess homogenous adhesion properties. Occasionally, small aggregates of 2~3 neurons were observed, suggesting that neurons form clusters early in cell culture, possibly because of poor adhesion properties of the surface (proto-clusters). Indeed, all MWNT-A surfaces (MWNT-A_0 to MWNT-A_5) presented cell densities that are smaller than that observed for primary cultures on PDL-coated coverslip (respectively, 77 ± 7, 64 ± 11, 59 ± 7, 52 ± 11, 201 ± 19 and 69 ± 15 cells/mm^2) suggesting that many cells fall off the surface because of poor adhesion properties. These values however inform us that MWNT-A_4 is the best surface for cell adhesion and is closely comparable to coverslips with PDL. Interestingly, the surfaces of the various MWNT-A differ in their ability to promote neuronal differentiation. The morphology of neurons grown on MWNT-A_4 mostly resembles that of neurons grown on PDL-coated coverslip (number of neurites and length, data not shown). Conversely, neuronal differentiation is less developed on

MWNT-A_0 , MWNT-A_1 , MWNT-A_2 and MWNT-A_3 (shorter and fewer neurites). Nevertheless, the percentage of neurons over the entire cell population remains in a similar range (65% for MWNT-A_0 , 57% for MWNT-A_1 , 61% for MWNT-A_2 and 43% for MWNT-A_3 compared to 59% for MWNT-A_4). Interestingly, these values indicate that none of these surfaces select one cell type over the other one (i.e. glial cells do not develop faster, or these substrates do not produce selective cell toxicity). In that respect, MWNT-A_5 differed dramatically from other chemistries. Neurons show little differentiation/development (absence of neurites) and the percentage of neurons is much smaller (10%) presumably because progenitors did not differentiate into the neuronal phenotype. The excellent cell adhesion and neurite outgrowth observed on MWNT-A_4 is surprising considering that this surface contains carboxyl groups which can deprotonate at pH 7.4 into negative COO^- groups, a factor that is non favorable to cell adhesion according the results observed for MWNT-A_2 surface and earlier reports [33]. We believe that the drastic difference observed between MWNT-A2 and MWNT-A4 is due to a higher hydrophilicity of the MWNT-A4 surface (lower water angle) and the presence of OH groups that may engage hydrogen bonds with negatively charged COO^- groups of cell surface proteins.

Cultured neurons on MWNT-A after 8 days in vitro

The state of differentiation of neurons is incomplete at 3 DIV. Therefore, we also imaged and analyzed the outcome of cell cultures on MWNT-A at 8 DIV, a stage where neurons are far more mature with regard to electrical activity and synaptic connections (figure 3). This increased state of differentiation is well illustrated on PDL-coated coverslip (see figure S2(B)). On that surface, neuronal maturation is witnessed by a considerable increase in the number and length of neurites that creates a seemingly disorganized network of connections. Also, neurons are mostly individual and restricted soma clustering is observed. The neuronal phenotypes present on two MWNT-A surfaces merit immediate comments. Similar to 3 DIV, neurons still lack neurites at 8 DIV on the MWNT-A_5 surface (figure 3(A)). Also, neurons still represent 9% of total cell population at 8 DIV, a value closely similar to 3 DIV, suggesting that no neuronal differentiation occurs on this surface, even after prolonged time in culture. This is an expected finding that indicates that the PEG_{5000} covalently functionalized surface has too little adhesion properties to favor cell clustering and neurite extension. The lack of neurite extension also implies that neurites cannot form bundles or fascicles independently of the support. Such a surface might be of interest to the investigator who would like to study to force neurons to remain in a non-differentiated state. Neurons grown on MWNT-A_4 showed little evolution at 8 DIV (figure 3(B)) compared to 3 DIV (figure 2(E)) except that, like on PDL-coated coverslips (figure S2(B) in supplementary information), neurites were more abundant and of greater length. Similarly, the network of neurites is also anarchical in its organization. We conclude the MWNT-A_4 surface resembles the most PDL-coated coverslips for neuronal maturation.

In sharp contrast to MWNT-A_4 and MWNT-A_5 , the organization of neurons on MWNT-A_0 , -A_1 , -A_2 and -A_3 surfaces differs dramatically between 3 DIV and 8 DIV (figure 3(C-F)). Neurons showed clear signs of aggregation by forming large somatic clusters and a great proportion of the neurites organize into fascicles. A SEM study to investigate the shape of the neuronal clusters indicates that neurons organize into three-dimensional clusters of tens of neurons (figure 4(A,B)). Most of these clusters have sphere-like structures. We measured the average cluster diameter and density, and the average inter-cluster distance on each MWNT-A (-A_0 to -A_3) surface. The average cluster diameters are similar for all substrates (figure 5(A)). Average diameters may be slightly over-estimated in some conditions (for instance MWNT-A_3 , Figure 3F) due to the fact that small clusters were discarded from the analyses (see methods). Noteworthy, this observation leads to three remarkable conclusions: i) neurons have the ability to migrate on the substrate and to form clusters before immobilization once a critical size has been reached during the period of time between 3 DIV and 8 DIV; ii) clusters should contain similar cell densities; and iii) the formation of clusters indicates that cell/cell interactions are favored over cell/substrate interactions for MWNT-A_0 to MWNT-A_3 substrates, which is presumably not the case for the MWNT-A_4 substrate. The densities of the neuronal clusters were also closely similar between the different MWNT-A substrate (18 clusters/mm^2), except for the MWNT-A_3 substrate (12 clusters/mm^2) (figure 5(B)). This difference is most likely related to the lower adhesion properties of neurons on PEG_{5000} -functionalized surface as measured at 3 DIV. Next, we determined the average distance of inter-connected clusters for the substrates on which clusters and fascicles of neurites were observed. As shown, the surfaces differed by their ability to support long inter-connections between clusters (figure 5(C)). The best surface was MWNT-A_0 with an average interconnected cluster distance of 249 ± 18 μm. This value is lower on the MWNT-A_1 and MWNT-A_2 surfaces (210 ± 14 μm and 194 ± 11 μm, respectively). The poorest surface was MWNT-A_3 with an average inter-connected cluster distance of 147 ± 9 μm. We conclude from this analysis that these surfaces differ sufficiently in their strength of cell/surface interaction to influence cluster inter-connecting neurite bundle lengths.

The propensity of neurons to organize into clusters on the various MWNT-A surfaces indicates that bundle organization obeys to the same basic rule: i.e. preferred neurite/neurite interaction over neurite/surface interaction. Several measures were performed to illustrate this point using only MWNT-A_0 to -A_3 , since these surfaces are most concerned by the clustering behavior (figure 6). All surface chemistries favored the formation of neurite fascicles (figure 6(A)). For MWNT-A_0 , MWNT-A_1 and MWNT-A_2 , more than 90% of the neuronal clusters produced neurite fascicles that exit the clusters. This observation implies that these chemical surfaces present enough cell adherence properties to facilitate neurite extension and neurite escape from the neuronal cluster spheres. In sharp contrast, only 40% of neuronal clusters have the ability to produce outgoing neurite fascicles on MWNT-A_3 surface. This result indicates that neurites probably prefer in many cases to stay in the neuronal cluster environment rather than exiting the cluster. This observation would be in agreement

with the observation that this PEG_{5000} -functionalized surface reduces also the density of the clusters compared to the other surface chemistries. Examining the number of neurite fascicles that emerge from neuronal clusters gives coherent results (figure 6(B)). Values are close to 3–5 neurite fascicles on all MWNT-A chemistries for neuronal clusters that have the ability to produce outgoing neurite fascicles. The smallest value is found for MWNT-A_1 chemistry (close to 3 neurite fascicles exiting from the clusters), most likely because this surface chemistry also allows the emergence of individual neurites. This value is maybe underestimated owing to the fact that small fascicles, easy to confuse with individual neurites, were discarded as classified as fascicle from our analyses. The ratio of neurite fascicles over individual neurites is illustrated in more details in figure 6(E, F) . Most importantly, we observed that surface chemistries differed dramatically with regard to the percentage of neurite fascicles that have the ability to connect a neuronal cluster different from the one from which it originates (figure 6(C)). The best surface for inter-cluster connection and network organization is without any doubt MWNT-A_0 since 100% of the neurite fascicles connect another neuronal cluster. In contrast, neurons grown on MWNT-A_3 have the lowest percentage of inter-cluster connection (close to 10% only). For the three surface chemistries that possess fascicles failing to inter-connect to different neuronal clusters (MWNT-A_1 , -A_2 and -A_3), the average length of non-connecting neurite fascicles is close to 100 μm (figure 6(D)), except for neurite fascicles that emerge from neuronal clusters grown on MWNT-A_3 probably because of the furtive nature of the PEG_{5000} -functionalized surface. This reduced length of neurite fascicles may explain the weak success rate of inter-cluster connection observed with this chemistry. Finally, we investigated the ratio between outgoing neurite fascicles and individual neurites. Figure 6(E) illustrates confocal microscopy stack images of representative neuronal clusters grown on MWNT-A_0 , MWNT-A_1 and MWNT-A_2 . These images show that MWNT-A_0 favors the formation of neurite fascicles over individual neurites, but that neurite organization within the bundle is loose. This organization is further loosened for neurites emerging from neuronal clusters grown on MWNT-A_1 . Finally, the neurite fascicles that grow on MWNT-A_2 chemistry show close proximity of neurites. This probably explains why there is a low percentage of individual neurites that emerge from the neuronal clusters with this chemistry. The neurite fascicles to individual neurites ratio are quantified in figure 6(F) and support these observations. Overall, these data demonstrate that surface chemistry of MWNT-A has the potential to largely weight on the cellular architecture originating from the neuronal clusters. For clusters grown on MWNT-A_0 , -A_1 , -A_2 and -A_3 , we refer to network-like, sunshine-like, fractal-like and ball-like neuronal clusters, respectively (figure 3(C-F) , figure 6(E)).

MWNT-A functionalisation influences patterning of neurons

Our work illustrates that the surface chemistry of MWNT-A greatly influences neuronal behavior and differentiation. We have showed that the supports are biocompatible and non toxic to neurons, but that the cell adhesion properties are low enough so that cell motility and cluster formation is possible. We therefore investigated how neurons would behave if choice was given between two different chemistries on the same support. We developed mixed MWNT-$A_{4/5}$ surfaces with one half side treated with plasma oxygen, and the other half with plasma oxygen plus PEG_{5000} . PEG_{5000} surface do not allow neuronal differentiation and clustering, whereas conversely, plasma oxygen-treated surface allows extensive differentiation without clustering owing to better cell adhesion properties. Figure 7(A) illustrates the extensive neuronal differentiation and neurite outgrowth on the plasma oxygen-treated surface at 8 DIV, whereas neurons were almost not differentiated and very rare with the additional PEG_{5000} treatment. The low neuronal density on the PEG_{5000} -treated surface illustrates its weaker cell adhesion properties and/or the motility of neurons towards the plasma-oxygen-treated surface. Interestingly, the extensive neurite network of the plasma-treated surface does not extend into the PEG_{5000} -treated surface according to the line of separation. We also investigated whether substrate-preference for neuronal maturation could also occur if both chemistries were less drastically different. Similar MWNT-$A_{0/2}$ surfaces were developed and investigated with regard to neuronal development at 8 DIV (figure 7(B)). Neurons again developed a preference for a given substrate, here the non-functionalized surface. Indeed, as we can see from the above results, both surfaces taken individually have the same cell density at 3 DIV and identical cluster densities at 8 DIV (~18 neuronal clusters/mm^2). But on the MWNT-$A_{0/2}$ surface, cluster density on the MWNT-A_2 side dropped down to 6/mm^2 at the interface with the MWNT-A_0 side indicating again that neuronal motility occurs in order to enrich the MWNT-A_0 surface. At a distal distance of the interface, cluster density on MWNT-A_2 again increases to values close to 18/mm^2 (data not shown). These results lead to two conclusions: i) it is possible to orient the migration of neurons on a given surface with appropriate chemical treatment of MWNT-A, and ii) developing MWNT-A surface with double chemistries allows for neuronal substrate preference classification. Since neurons display preferential substrate attachment and oriented maturation, we investigated whether we could influence cell morphology by micro-patterning (figure 7(C-E)). Needle scratches of 5 to 10 μm width were performed on MWNT-A_5 substrates in order to form TiN-exposed gutters (MWNT-A_{5S}) and neuron development investigated after 8 DIV. SEM imaging illustrates that neurons prefer to grow and develop neurites within the TiN gutter in order to avoid the non-differentiating MWNT-A_5 surface (figure 7(C)). Neurites follow the gutter curvatures and the rare neurites that branch onto the MWNT-A_5 surface are blocked in their development (figure 7(D)). This observation is compatible with the fact that MWNT-A_5 surface inhibits neuronal differentiation (figure 3(A)). In contrast, when scratches were performed on MWNT-A_0 , a substrate highly compatible with neuronal differentiation, the opposite observation was made, i.e. neurons prefer to grow on the MWNT-A substrate rather than in TiN gutters. These data indicate that the neuronal growth we observed previously in gutters of the MWNT-A_5 substrates is not due to the topology of the surface, but to chemical differences of the substrate. Overall, these data indicate that micro-patterning of neuronal morphology is possible using MWNT-A and differential chemical treatments.

Discussion

In summary, this study indicates that it is of interest to investigate the behavior of neurons at 8 DIV since it reveals unexpected collective neuronal responses towards the substrate. At 8 DIV, the collective neuronal responses differed among the various substrates ruling out a major contribution of sera protein deposition on substrate surface in modulating neuronal adhesion, migration and neurite extension. On MWNT-A_0 , neurons develop network-like neuronal clusters providing images that contrast with classical cultures by enhanced clustering of neuronal soma and the formation of neurite fascicles. This tends to indicate that after a certain time in vitro after cell seeding at the surface, neurons have the ability to migrate and gradually prefer a neuron/neuron interaction over the initial neuron/substrate interaction that occurs immediately after seeding and before neurite extension. Since this behavior also applies to neurite extension creating neurite fascicles between clusters of neurons, this property may find desirable applications when it comes to study cell/cell communication on a collective scale rather than through individual neuron connections as occurring on classical substrates. In addition, neurite extension and connections between clusters of neurons appear less chaotic than on PDL-treated surface suggesting that connectivity may be rationalized and directed. Interestingly, we demonstrate that altering the relative affinity between neuron/neuron and neuron/substrate through chemical functionalization allows the appearance of several new neuronal organizations. A similar conclusion was reached in an earlier study [34]. The differences in contact angles with H_2O, that reveal differences in surface hydrophobicity, offer a possible explanation as to why neurons aggregate differently on the various substrates. Also, the natures of the chemical groups immobilized at the various surfaces are likely to play an important role.

Cell cultures can evolve in one of two directions. Plasma oxygen treatment enhances neuron/substrate interaction and hence diminishes neuronal cluster and neurite bundle formation to the point that the culture resembles classical neuronal cultures on PDL-coated coverslips. Whereas, PEG_{5000} -treatment as performed for MWNT-A_5 produces exactly the opposite behavior: complete lack of neuronal differentiation although cells appear to survive well on the support. The concomitant lack of neuronal clustering is probably due to the complete absence of neurites on this surface. Indeed, neurites are thought to favor cell motility of the surface which is required for the clustering [35 –37]. Other chemistries produce intermediate phenotypes, including MWNT-A3, probably because PEG_{5000} functionalization is lower or the coupling strategy different. These chemistries reduce cell adherence but do not block neurite formation. Hence cell clustering and bundle formation is intact. However, these chemistries can be differentiated by their ability to sustain the adherence of individual neurites and their control of neurite bundle length. These differences in cell adhesion translate into the late formation of clusters of various shapes such as fractal-like, sunshine-like and ball-like. The morphological differences observed in the networks may have interesting applications. The ball-like network of MWNT-A_3 chemistry is characterized by an almost complete absence of inter-cluster connection and the 3D growth of a neurosphere implying privileged cell to cell contacts over cell to surface contacts. Such a property may be highly desirable for oncology in studies aiming at characterizing compounds that prevent cell to cell adhesion and proliferation.

Chemical functionalisation of MWNT-A substrate also appears as an asset when it comes to micro-patterning. A similar conclusion was reached earlier in a study where authors showed that neurites from hippocampal neurons extended preferentially along poly-L-lysine treated CNT-based pattern [38]. Obviously, the differential affinity of neurons for different chemistries turns out to be advantageous if the objective is to control the location of neuronal development and neurite extension. It is also of interest to develop mixed chemical surfaces to investigate cell migration properties and cell adherence preferences. For the first time, our study paves the way for further investigations on the influence of chemical treatment of MWNT-A in the collective organization and patterning of neurons.

Ackowledgements:

We thank Dr Isabelle Marty (Inserm U836, Grenoble, France) for the use of the confocal microscope. O.B. is a PhD student from CEA. J.L. has a postdoctoral fellowship of CEA. We acknowledge financial support of Inserm (F.A. and M.D.W.) and of CEA Leti (F.S.S. and G.M.). The silicon chips were processed by the CEA Leti in the Minatec clean room. We also thank Jean Dijon and Hélène Le Poche (CEA Liten) for the growth of carbon nanotubes.

Footnotes:

Supplementary Data Supplementary data on detailed characterization of functionalized MWNT-A, and fluorescence microscopy images of neurons cultured on PDL-coated coverslips after 3 and 8 DIV.

References:

- 1 . Vidal JJ . 1977 ; Real-time detection of brain events in EEG . Proceed IEEE . 65 : 633 - 41
- 2 . Lebedev MA , Nicolelis MAL . 2006 ; Brain-machine interfacing: past, present and future . Trends Neurosci . 29 : 536 - 46
- 3 . Stanley GB . 1999 ; Reconstruction of natural scenes from ensemble responses in the LGN . J Neurosci . 19 : 8036 - 42
- 4 . Wessberg J . 2000 ; Real-time prediction of hand trajectory by ensembles of cortical neurons in primates . Nature . 408 : 361 - 5
- 5 . Benabid AL . 1991 ; Long-term suppression of tremor by chronic stimulation of the ventral intermediate thalamic nucleus . Lancet . 337 : 403 - 6
- 6 . Keefer EW . 2008 ; Carbon nanotube coating improves neuronal recordings . Nat Nanotech . 3 : 434 - 9
- 7 . Sauter-Starace F . 2009 ; ECoG recordings with carbon nanotubes electrodes of a flexible Polyimide implant in non-human primate . IEEE EMBS . 2009 4th neural engineering Minnesota, USA
- 8 . Bekyarova E . 2005 ; Applications of carbon nanotubes in Biotechnology and Biomedicine . J Biomed Nanotech . 1 : 3 - 17
- 9 . Harrison BS , Atala A . 2007 ; Carbon nanotube applications for tissue engineering . Biomaterials . 28 : 344 - 53

- 10 . Silva GA . 2006 ; Neuroscience nanotechnology: progress, opportunities and challenges . Nat Rev . 7 : 65 - 74
- 11 . Georges PC . 2006 ; Matrices with compliance comparable to that of brain tissue select neuronal over glial growth in mixed cortical cultures . Biophys J . 90 : 3012 - 18
- 12 . Zuidema JM . 2010 ; Fabrication and characterization of tunable polysaccharide hydrogel blends for neural repair . Acta Biomaterialia . 10.1016/j.actbio.2010.11.039
- 13 . Carrero-Sanchez JC . 2006 ; Biocompatibility and toxicological studies of carbon nanotubes doped with nitrogen . Nano Lett . 6 : 1609 - 16
- 14 . Poland CA . 2008 ; Carbon nanotubes introduced into the abdominal cavity of mice show asbestos-like pathogenicity in a pilot study . Nat Nanotech . 3 : 423 - 8
- 15 . Dubin RA . 2008 ; Carbon nanotube fibers are compatible with mammalian cells and neurons . IEEE Trans Nanobiosci . 7 : 11 - 4
- 16 . Cheng C . 2009 ; Toxicity and imaging of multi-walled carbon nanotubes in human macrophage cells . Biomaterials . 30 : 4152 - 60
- 17 . Ciofani G . 2010 ; In vitro and in vivo biocompatibility testing of functionalized carbon nanotubes . Methods Mol Biol . 625 : 67 - 83
- 18 . Mazzatenta A . 2007 ; Interfacing neurons with carbon nanotubes: electrical signal transfer and synaptic stimulation in cultured brain circuits . J Neurosci . 27 : 6931 - 6
- 19 . Galvan-Garcia P . 2007 ; Robust cell migration and neuronal growth on pristine carbon nanotube sheets and yarns . J Biomater Sci Polym Ed . 18 : 1245 - 61
- 20 . Lovat V . 2005 ; Carbon Nanotube Substrates Boost Neuronal Electrical Signaling . Nano Lett . 5 : 1107 - 10
- 21 . Gabay T . 2007 ; Electro-chemical and biological properties of carbon nanotube based multi-electrode arrays . Nanotech . 18 : 035201 -
- 22 . Saito N . 2009 ; Carbon nanotubes: biomaterial applications . Chem Soc Rev . 38 : 1897 - 903
- 23 . Cellot G . 2009 ; Carbon nanotubes might improve neuronal performance by favouring electrical shortcuts . Nat Nanotech . 4 : 126 - 33
- 24 . Hu H . 2004 ; Chemically functionalized carbon nanotubes as substrates for neuronal growth . Nano Lett . 4 : 507 - 11
- 25 . Mattson M . 2000 ; Molecular functionalization of carbon nanotubes and use as substrates for neuronal growth . J Mol Neurosci . 14 : 175 - 82
- 26 . Xie J . 2006 ; Somatosensory neurons grown on functionalized carbon nanotube mats . Smart Mater Struct . 15 : N85 - 88
- 27 . Hu H . 2005 ; Polyethyleneimine Functionalized Single-Walled Carbon Nanotubes as a Substrate for Neuronal Growth . J Phys Chem B . 109 : 4285 - 9
- 28 . Malarkey EB . 2009 ; Conductive Single-Walled Carbon Nanotube Substrates Modulate Neuronal Growth . Nano Lett . 9 : 264 - 8
- 29 . Liu J . 2009 ; Stable non-covalent functionalisation of multi-walled carbon nanotubes by pyrene-polyethylene glycol through pi-pi stacking . New J Chem . 33 : 1017 - 24
- 30 . Nakashima N . 2002 ; Water-Soluble Single-Walled Carbon Nanotubes via Noncovalent Sidewall-Functionalization with a Pyrene-Carrying Ammonium Ion . Chem Lett . 638 - 9
- 31 . Guldi DM . 2005 ; Functional single-wall carbon nanotube nanohybrids associating SWNTs with water-soluble enzyme model systems . J Am Chem Soc . 127 : 9830 - 8
- 32 . Banker G . 1998 ; Rat Hippocampal Neurons in Low-Density Culture . 2 MIT press ;
- 33 . Li B . 2005 ; Influence of carboxyl group density on neuron cell attachment and differentiation behavior: gradient-guided neurite outgrowth . Biomaterials . 26 : 4956 - 63
- 34 . Nichols AJ . 2008 ; Comparison of slow and fast neocortical neuron migration using a new in vitro model . BMC Neurosci . 9 : 50 -
- 35 . Song H , Poo M . 2001 ; The cell biology of neuronal navigation . Nat Cell Bio . 3 : E81 - 8
- 36 . Liang S , Crutcher KA . 1993 ; Movement of embryonic chick sympathetic neurons on laminin in vitro is preceded by neurite extension . J Neurosci Res . 36 : 607 - 20
- 37 . Marin O . 2006 ; Neurons in motion: same principles for different shapes? . Trends Neurosci . 29 : 655 - 61
- 38 . Jang MJ . 2010 ; Directional neurite growth using carbon nanotube patterned substrates as a biomimetic cue . Nanotechnology . 21 : 235102 -

Figure 1

(A) Schematic illustration of a cross-section of MWNT-A synthesized on Si substrate. (B) SEM images taken from a side view (upper panel) and top view (lower panel) of MWNT-A_0 . (C) Schematic illustration of the outermost graphene sheet of functionalized MWNT-A showing the different grafted molecules for each chemically-modified MWNT-A (in red).

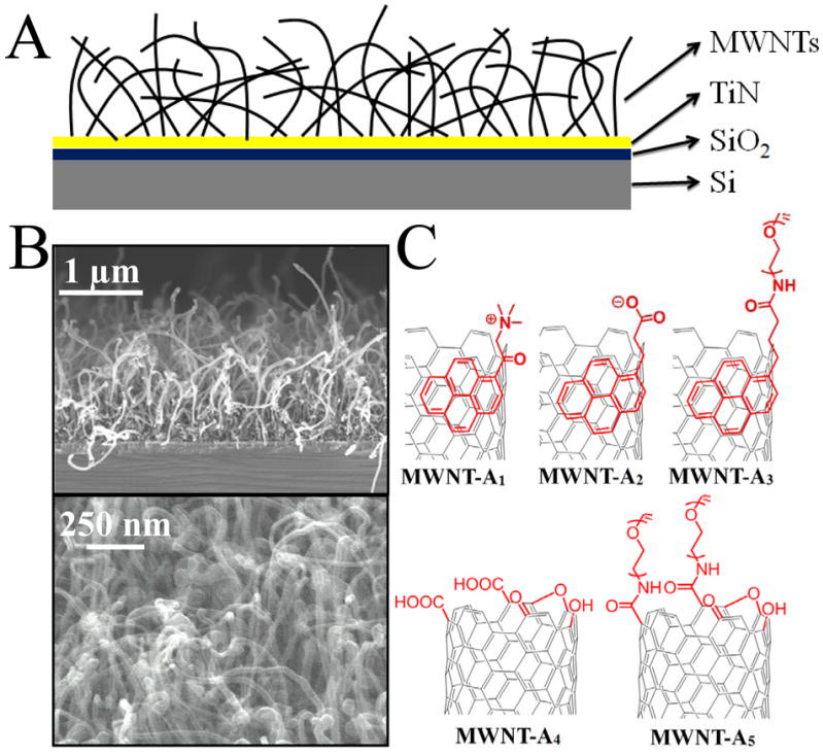


Figure 2

Fluorescent confocal microscopy of hippocampal cells at 3 DIV on (A) MWNT-A_5 , (B) MWNT-A_4 , (C) MWNT-A_0 , (D) MWNT-A_1 , (E) MWNT-A_2 and (F) MWNT-A_3 . Green labelling represents neuronal cytoskeleton marked by Tuj-1 tagged with Alexa488 (neurons only), and the red labelling shows nuclei staining by To-Pro3® (neurons and glial cells). The yellow colour arises from superimposition of red and green colours. Bar: 250 μm.

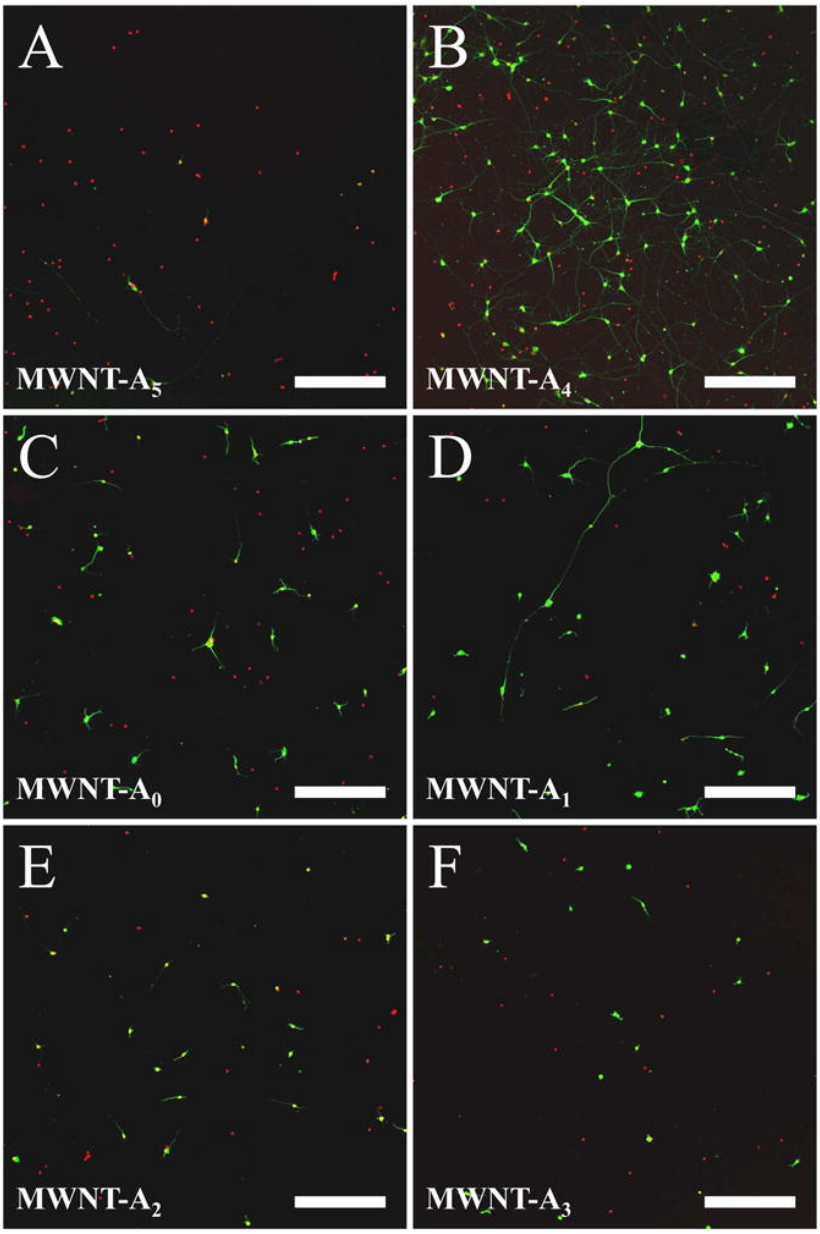


Figure 3

Fluorescent confocal microscopy images of hippocampal neurons at 8 DIV on raw and functionalized MWNT-A surfaces. (A) Non-differentiated neurons on MWNT-A_5 substrate. (B) Classical neuronal network composed of individual neurons and neurites on MWNT-A_4. (C) Network-like neuronal cluster structure illustrating the numerous neurite fascicles inter-connecting the clusters on MWNT-A_0. (D) Sunshine-like neuronal cluster structure on MWNT-A_1. (E) Fractal-like neuronal clusters on MWNT-A_2. (F) Ball-like neuronal cluster on MWNT-A_3. Bar: 250 μm.

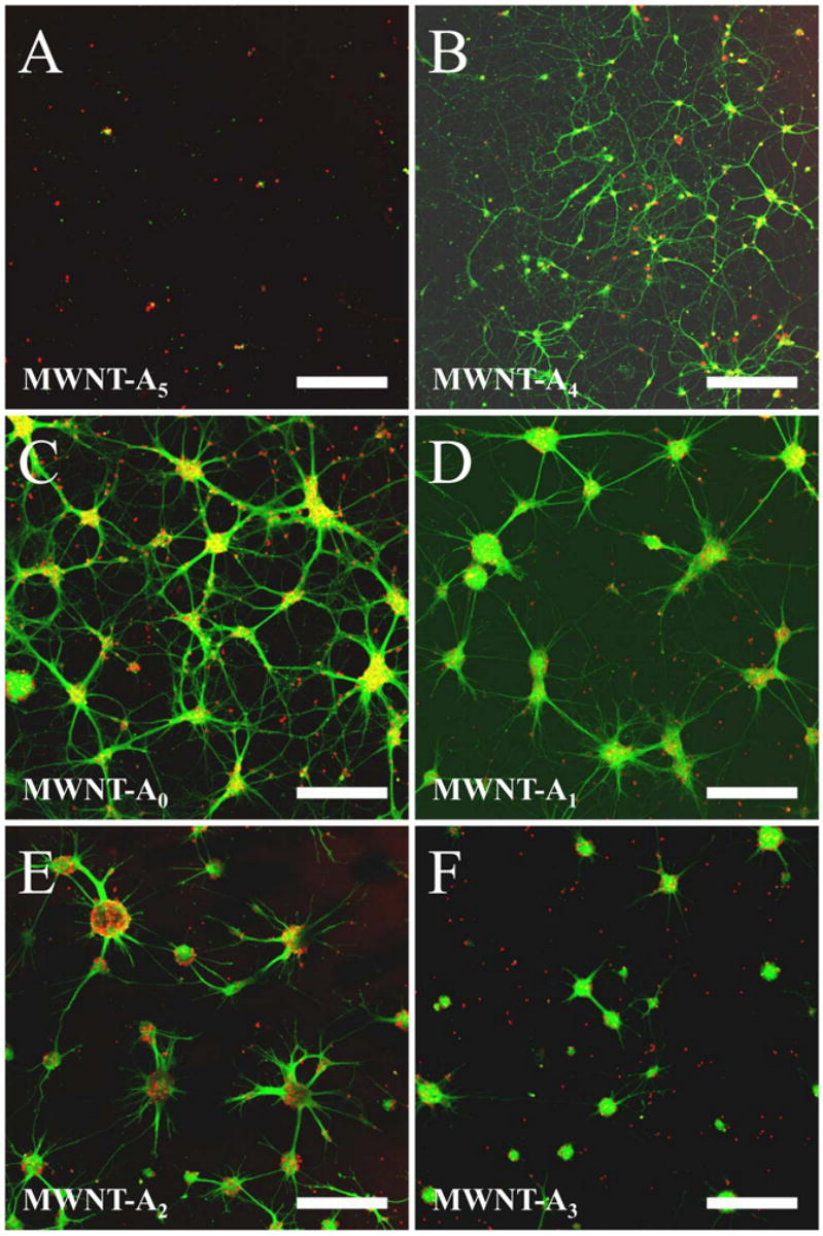


Figure 4

(A) SEM image of neuron clusters on MWNT-A_0 surface. (B) Zoom on a neuron cluster.

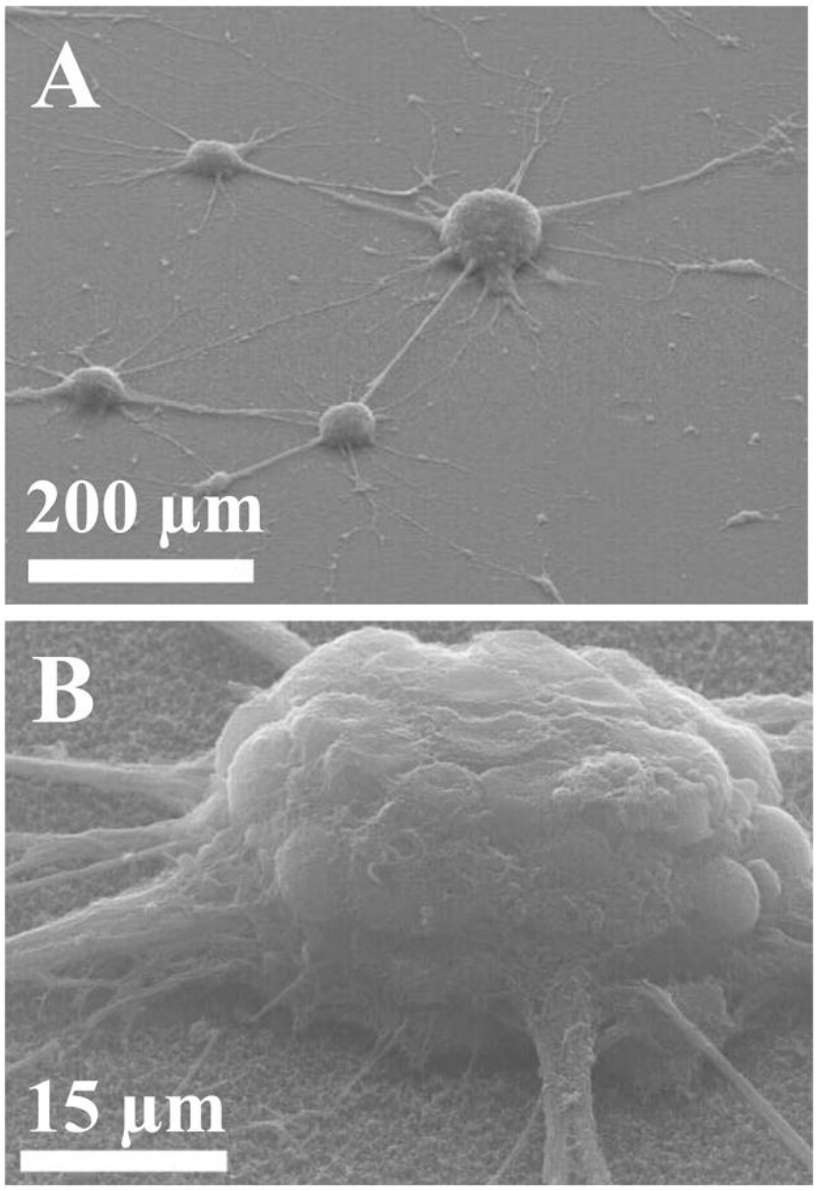


Figure 5

Comparison of the (A) diameter, (B) density of neuron clusters, and (C) inter-connected cluster distances on MWNT-A surfaces (-A_0 to A_3). Errors bars are s.e.m. Numbers in parentheses indicate the number of clusters studied in each condition. Asterisks indicate significant differences (* $p \leq 0.1$, ** $p \leq 0.05$, *** $p \leq 0.01$).

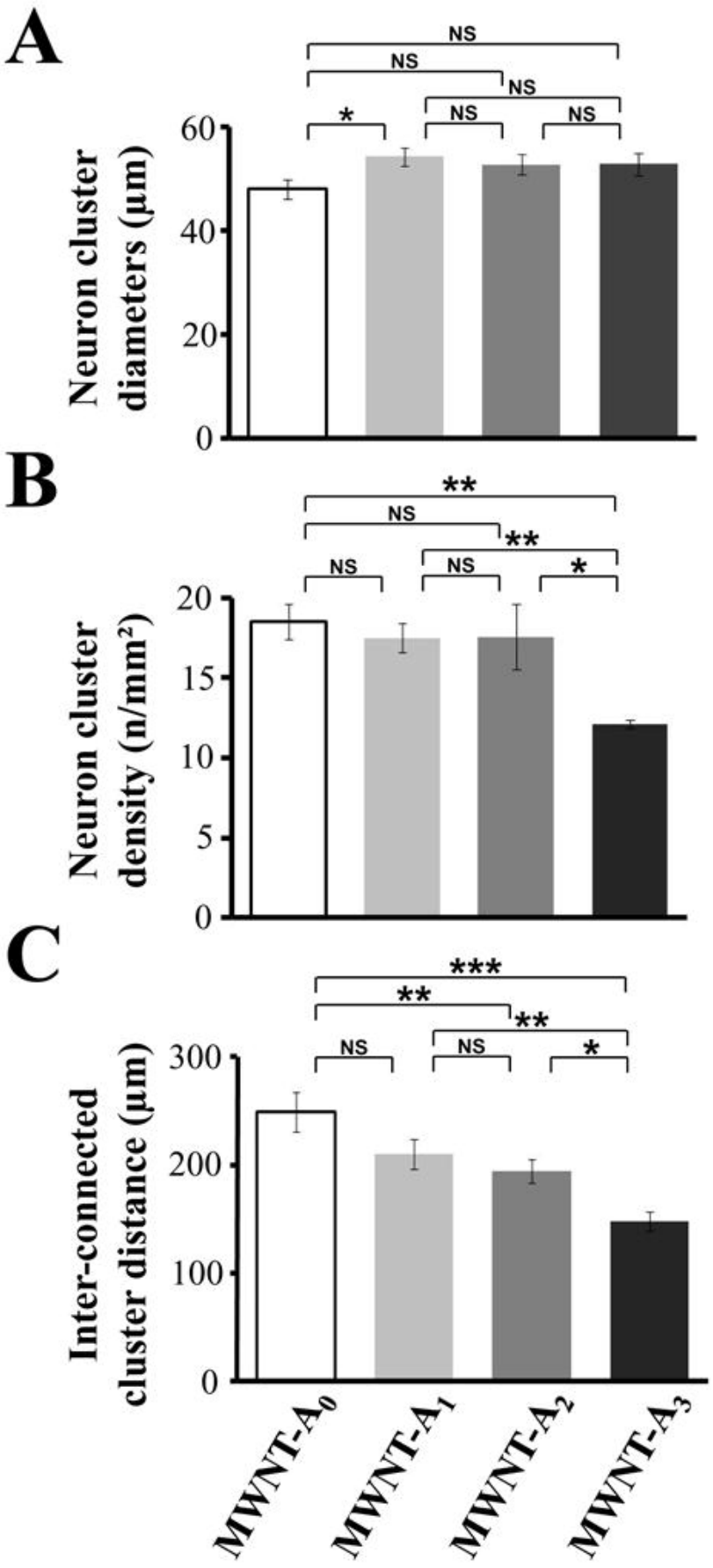


Figure 6

Organization of neurites originating from neuronal clusters. (A) Percentage of neuron clusters with neurite fascicles. (B) Average number of neurite fascicles emerging from neuronal clusters that possess neurite fascicles. (C) Percentage of neurite fascicles that inter-connect neuronal clusters. (D) Average length of neurite fascicles that do not connect another neuronal cluster. (E) Stack images from confocal microscopy of representative neuronal clusters illustrating cluster-emerging neurite organization. Green is Tuj-1 Alexa488 labeling and red is To-Pro3 staining. (F) Ratio between neurite fascicles over individual neurites for each MWNT-A chemistry. Errors bars are s.e.m. Numbers in parentheses indicate the number of clusters or neurite fascicles studied in each condition. Asterisks indicate significant differences (* $p \leq 0.05$, ** $p \leq 0.01$, *** $p \leq 0.001$).

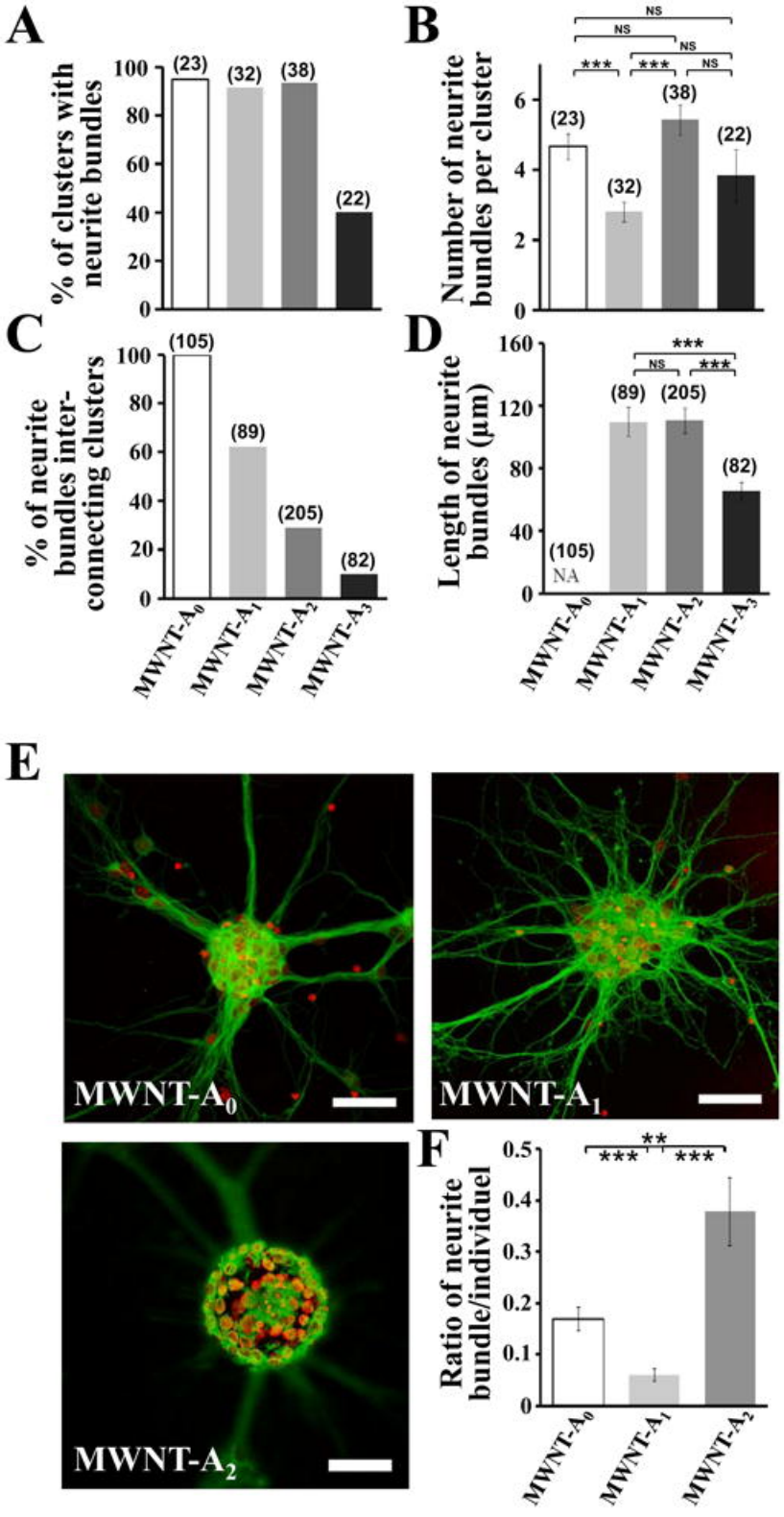


Figure 7

Substrate differences for neuronal maturation. Confocal microscopy images on MWNT-$A_{4/5}$ (A) and MWNT-$A_{0/2}$ (B) surfaces illustrating the substrate preference of neurons. Dashed lines mark the interface between two different chemical functionalisations. Bar: 250 μm. (C) SEM image illustrating the preferential growth of neurons and neurites into a TiN gutter made on MWNT-A_5 . (D) Magnification of image shown in (C) confirming the preferential attachment and development of neurites in the TiN gutter. (E) Absence of neuronal growth in TiN gutter made on MWNT-A_0 substrate.

